Atmospheric Linke Turbidity Index over Deukhuri Valley, Dang

P. M. Shrestha, S. P. Gupta, U. Joshi, N. P. Chapagain, I. B. Karki, and

K. N. Poudyal

Journal of Nepal Physical Society
Volume 8, No 2, 2022
(Special Issue: ANPA Conference 2022) ISSN: 2392-473X (Print), 2738-9537 (Online)

JNPS, **8** (2), 1-6 (2022)
DOI: http://doi.org/10.3126/jnphyssoc.v8i2.50136

Published by: Nepal Physical Society
P.O. Box: 2934
Tri-Chandra Campus
Kathmandu, Nepal
Email: nps.editor@gmail.com

ANPA Conference 2022
ISSN : 2392-473X(Print), 2738-9537 (Online)

Research Article ©Nepal Physical Society
DOI:http://doi.org/10.3126/jnphyssoc.v8i2.50136

Atmospheric Linke Turbidity Index over Deukhuri Valley, Dang

P. M. Shrestha,[1,2] S. P. Gupta,[1,a)] U. Joshi,[1,2] N. P. Chapagain,[3] I. B. Karki,[1] and K. N. Poudyal[4]

[1)]*Department of Physics, Patan Multiple Campus, IoST, Kathmandu Nepal*
[2)]*Central Department of Physics, IoST, Kritipur Nepal*
[3)]*Department of Physics, Amrit Campus, IoST, Kathmandu Nepal*
[4)]*Department of Physics, Pulchowk, IoST, Kathmandu Nepal*

[a)]*Corresponding author: suresh.gupta@pmc.tu.edu.np*

Abstract. The aim of this project is to study Atmospheric Linke turbidity index over Deukhuri Valley, Dang (27^o50'32.2" N, 82^o45'41.9" E and 445 m a. s. l.). The atmospheric Linke Turbidity index is calculated from solar radiation measurements of NASA satellite for period of 4 years (2015, 2016, 2017, 2018). The annual average clearness index (K_T), Linke turbidity index (L_T) and visibility are 0.55 $\pm$ 0.12, 2.5 $\pm$ 1.1 and 10.4 $\pm$ 3.8 km respectively. Atmospheric Linke turbidity index is used on agriculture, hydrology, climate change and energy harvesting. In study period, number of good days (visibility $>$ 15 km) and number of bad days (visibility $<$ 5 km) are found to be 188 and 94 respectively. This research work is beneficial for the further identification, impact and analysis of atmospheric turbidity at different places.

Received: 08 August 2022 ;**Accepted**: 30 October 2022; **Published**: 31 December 2022

Key words: Atmospheric turbidity, clearness index, extinction coefficient, Linke turbidity.

INTRODUCTION

The Sun is the nearest star from the Earth. Solar energy is a clean, renewable and sustainable energy for solar energy applications around the world [1]. The quality and amount of solar radiation passing through the atmosphere is altered by atoms molecules like ozone, water vapor, carbon dioxide as well as by liquid and solid aerosols that are present along the propagation path. Solar radiation is usually influenced by three groups of dynamic factors: position of Sun and Earth position, terrain and atmospheric affects [2].

The geo-structure of Nepal is complex and for every 200m altitude there exist different climatic zones. This country is situated in the lap of the Himalaya and is landlocked situated between India and China with latitudes of 26.36^o N to 30.45^o N and longitudes of 80.06^o E to 88.2^o E. The elevation of the country ranges from 60 m to 8848 m above sea level all within the distance of 185 km wide [3]. Nepal lies in solar belt (15^o N to 35^o N). The annual average sunshine hour and solar energy are about 6.8 hours per day and 4.7 kWh/m^2/day in Nepal respectively [4]. In fiscal year 2018/19, 68.5 %, 29.4 % and 2.1 % of total energy consumption were conventional, commercial and renewable energy respectively. Total annual energy availability was 7,551.23 gigawatt hours. About 10.0 % of the total population have access to electricity from renewable energy sources [5]. Nepal is situated between two giant industrial countries India and China and their industrial byproduct can directly effect on the atmosphere. The atmospheric turbidity on Dang is needed to study.

Solar irradiance at ground level is highly dependent on the Earth's atmospheric turbidity. Atmospheric turbidity is a dimensionless measure of the opacity of a vertical column of the atmosphere. Atmospheric transparency can be affected both by natural phenomena within the Earth's atmosphere like clouds, dust, etc. and by human activity like factories, vehicles and many more [6]. Different parameters have been defined to evaluate the atmospheric turbidity to the attenuation of solar radiation reaching the Earth's surface and aerosols in the atmosphere [7]. The most common parameters used are Angstrom turbidity

(β) and Linke turbidity (L_T) [8]. Linke (1922) proposed to express the total optical thickness of a cloudless atmosphere as the product of two terms, the optical thickness of a water and aerosol free atmosphere and the Linke turbidity coefficient (L_T) [**?**]. These turbidity indices have been widely used at several places around the world based on solar irradiance measurements to quantify the effects of aerosols and air pollutants on degrading horizontal visibility and reducing the amount of solar radiation reaching the ground.

In this research, we studied Atmospheric Linke turbidity index over Deukhuri Valley, Dang. Study of the atmospheric turbidity index are used on agriculture, hydrology, climate change, energy harvesting.

MATERIALS AND METHODS

By Beer Lambert's law, direct normal solar irradiance on outer layer atmosphere (I_o) is decreased in the atmosphere due to absorption and scattering [9]. Then direct normal solar irradiance on ground(I_n) is [10] .

$$I_n = I_o e^{-km} \tag{1}$$

Ratio of I_n to I_o is clearness index(K_T). It is function of optical air mass (m, m_a) and extinction coefficient (k). Linke (1922) defined Linke turbidity factor (L_T) as the number of clean dry atmospheres required to reproduce the attenuation of extra-terrestrial radiation caused by the real atmosphere [11]. Linke turbidity factor (L_T) is ratio of total extinction coefficient(k) to extinction coefficient due to Rayleigh scattering(δ_r) [12].

$$L_T = \frac{ln(I_o/I_n)}{m\delta_r} \tag{2}$$

where

$$\delta_r = (6.6296 + 1.7513m_a - 0.1202m_a^2 +$$

$$0.0065m_a^3 - 0.00013m_a^4)^{-1} \tag{3}$$

$$m_a = \frac{P}{101325[cos\theta_z + 0.15(93.885 - \theta_z)^{-1.253}]} \tag{4}$$

where θ_z is solar zenith angle, m_a is absolute optical air mass(m) and P is atmospheric pressure at the place. Solar zenith angle depends on solar declination (δ), latitude (ϕ)of the place, solar hour angle (ω) and day number of year(n_d).

$$\theta_z = \cos^{-1}(sin\delta\ \sin\phi + \cos\delta\ \cos\phi\ \cos\omega) \tag{5}$$

$$\delta = 23.45\sin(\frac{2\pi}{365}(284 + n_d)) \tag{6}$$

Visibility in km is [13]

$$vis = \frac{3.912}{k} \tag{7}$$

Fourier series is used to analyze seasonal variation [14].

$$y_s = a_0 + a_1\cos(\frac{2\pi}{365}n_d) + b_1\sin(\frac{2\pi}{365}n_d) \tag{8}$$

where n_d is day number of year, for 1st January, it is 1 and for 31 December it is 365. a_o is offset and amplitude of seasonal component is $\sqrt{a_1^2 + b_1^2}$.
Daily data of clearness index are collected from NASA website bluehttps://power.larc.nasa.gov/data-access-viewer/ for year 2015, 2016, 2017, 2018. Open source software Python 3.7 software is used to analysis data and to plot graph. Standard error (SE) is used as error bar in graph. Data are presented in form of 'mean($\bar{x}$) $\pm$ standard deviation(σ)'. Coefficient of variance (CV) is used to check variability of data.

$$CV = \frac{\sigma}{\bar{x}} \times 100 \tag{9}$$

The first quartile (Q_1), second quartile (Q_2, median) and third quartile (Q_3) indicate 25%, 50% and 75% of data. Skewness (γ_1),kurtosis (γ_2) are used to analyze nature of distribution of data. When skewness and kurtosis are zero, distribution of data is normal(Gaussian).

$$\gamma_1 = \sqrt{\frac{\mu_3^2}{\mu_2^3}} \tag{10}$$

$$\gamma_2 = \frac{\mu_4}{\mu_2^2} - 3 \tag{11}$$

Here μ_2,μ_3 and μ_4 are second moment, third moment and forth moment about mean respectively [15].

Dang is a district of Province no. 5 located in the inner Terai of midwestern Nepal. Deukhuri Valley (27^{o}50'32.2" N, 82^{o}45'41.9" E) of the district is the second largest valley of Asia surrounded by Sivalik Hills and Mahabharata Range with altitude 88 to 445 m above sea level as shown in Figure 1. It covers 600 km^2 area. Maximum temperature is 26.5^{o}C in August and minimum temperature is 13^{o}C in January. The annual precipitation is 1494.4 mm according department of hydrology and meteorology. Population and population density of the district are 548,141 and 190 per square km respectively [16].

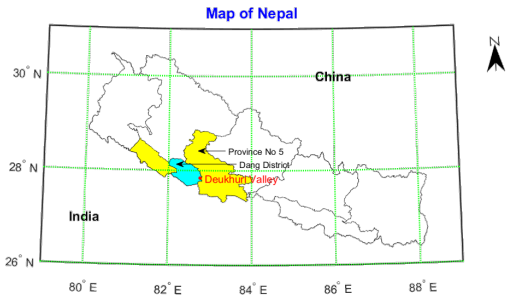

FIGURE 1. Map of Deukhuri, Dang [source: Survey Department, 2020]

RESULTS AND DISCUSSION

Daily data of clearness(K_T) are taken from NASA website and plot shown in Figure 2(a). The maximum value of clearness index is found 0.77 in 2015 March 10 due to clear day and the minimum value is found 0.09 in 2016 July 26 to cloudy day. During study period of 4 year, annual average of clearness index is 0.55 $\pm$ 0.12. Histogram of clearness index is shown in figure 3(a). The first quartile (Q_1), second quartile (Q_2, median) and third quartile (Q_3) of clearness index are found 0.48, 0.58 and 0.65 respectively. Skewness (γ_1) and kurtosis (γ_2) are found -1.08 and 1.05 respectively. Distribution of clearness index is negative tailed and is not normal. During study period of 4060 days, 507 days have clearness index between 0.6 to 0.7. Number of cloudy days (K_T < 0.34) and number of clear days (K_T > 0.65) are found 106 and 375 respectively [17]. Daily Linke turbidity (L_T) is calculated by using equation (1) and (2). Figure 2(b) shows daily variation of Linke turbidity. The maximum value of Linke turbidity is found 11.1 in 2015 February 28 due to large absorption and the minimum value is 1.1 in 2018 December 15 to less absorption.The during study period, annual average of Linke turbidity is 2.5$\pm$1.1. Histogram of Linke turbidity is shown in figure 3(b). The first quartile,second quartile and third quartile of Linke turbidity are found 1.8, 2.2 and 2.8 respectively. The skewness and kurtosis are found 2.64 and 10.42 respectively. Distribution of Linke turbidity is positively tailed and is not Gaussian. During study period of 4060 days, 829 days have Linke turbidity between 2 to 4. Daily visibility is calculated by using equation (1) and (3). Figure 2(c) shows daily variation of visibility (*vis*). The maximum value of visibility is found 23.3 km in 2015 October 2 due to clear day and the minimum value is 2.0 km in 2015 February 28 day due to fog. During study period, annual average is 10.4$\pm$3.8 km. Histogram of visibility is shown in figure 3(c). The first quartile, second quartile and third quartile of visibility are found 7.7 km, 10.0 km and 12.7 km respectively. The skewness and kurtosis are 0.46 and 0.02 respectively. Distribution of visibility is positively tailed and is not normal. During study period of 4060 days, During study period of 4060 days, 829 days have Linke turbidity between 2 to 4. days have Linke turbidity between 8 to 10 km. Number of bad days (visibility < 5 km) and number of good days (visibility > 15 km) are found 94 and 188 respectively [18].

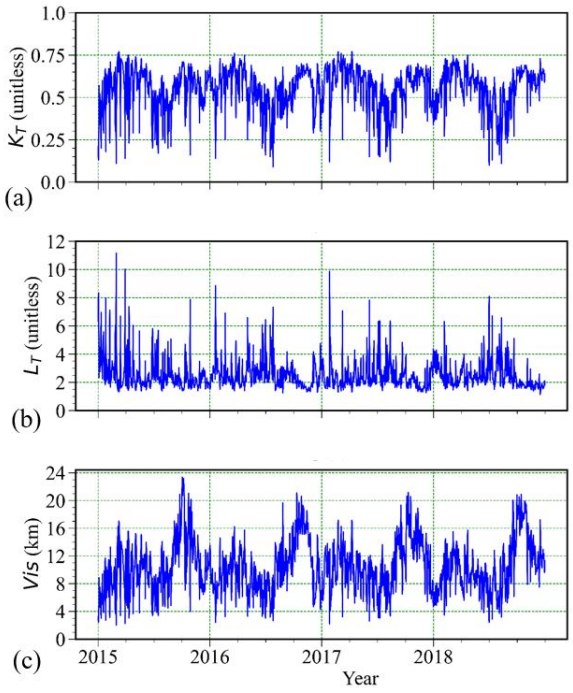

FIGURE 2. Daily variation of (a) clearness index, (b) Linke turbidity, and (c) visibility.

Figure 4(a) shows annual variation of clearness index (K_T). The maximum value of K_T is found 0.56$\pm$ 0.12 in 2017 having 104 clear days and minimum value is found 0.46$\pm$ 0.12 in 2016 having 87 clear days. K_T varies large in 2015 due to 24% coefficient of variance (CV) and less varies in 2016 due to 22% coefficient of variance. Figure 4(b) shows annual variation of Linke turbidity (L_T). Maximum value of L_T is 2.6$\pm$ 1.3 in 2015 and minimum value is 2.4$\pm$ 1.0 in 2017. In 2015, CV is large 50% and less 38% in 2018. Figure 4(c) shows annual variation of visibility. The maximum value of visibility is 10.6$\pm$ 3.6 in 2017 and minimum value is 10.2$\pm$ 3.7 in 2016. Visibility varies large in 39% coefficient of variance in 2015 and less in 34% coefficient of variance in 2017. Figure 5(a) shows monthly variation of clearness index (K_T). The maximum value of K_T is found 0.47$\pm$ 0.09 in March due to 82 clear day and minimum value is found 0.32$\pm$ 0.11 in July due to zero clear days. K_T varies large in July due to 35% coefficient of variance and less varies in November due to 9% coefficient of variance. Figure 5(b) shows monthly variation of Linke turbidity (L_T).The maximum

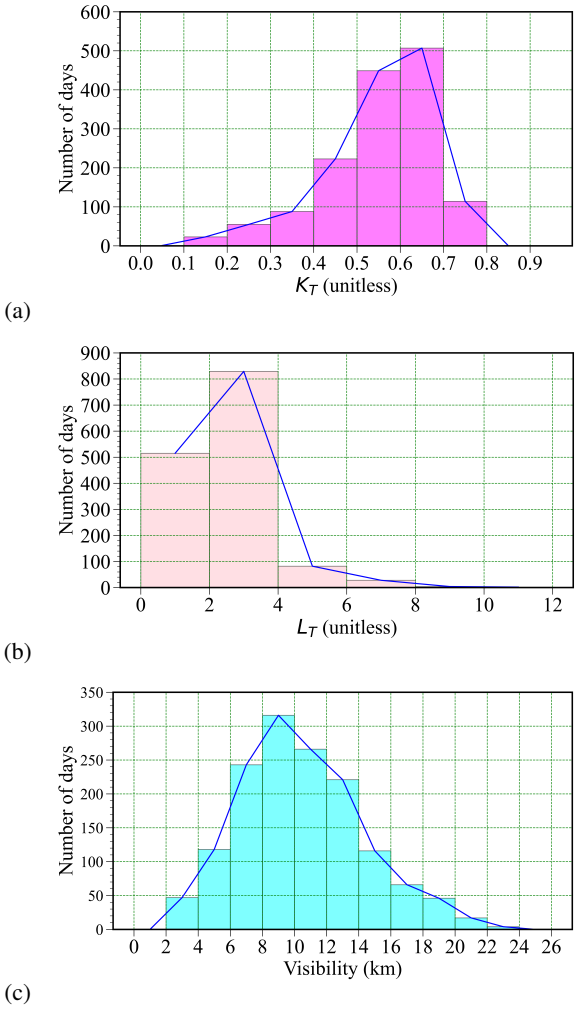

FIGURE 3. Histogram of (a) clearness index, (b) Linke turbidity, and (c) visibility.

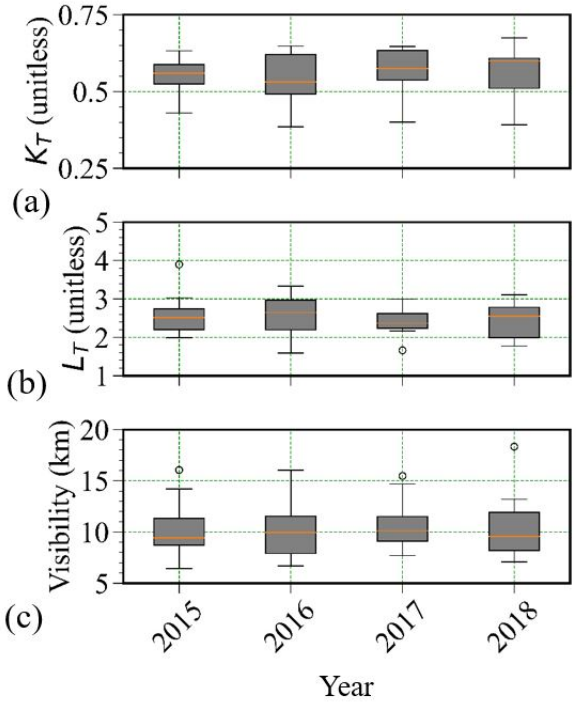

FIGURE 4. Annual variation of (a) clearness index, (b) Linke turbidity, and (c) visibility.

value of L_T is 3.2± 1.2 in January due to cloudy day and minimum value is 1.8± 0.3 in November due to clear day.L_T varies large in March due to 47% coefficient of variance and less in November due to 20% coefficient of variance. Figure 5(c) shows monthly variation of visibility. The maximum value of visibility is 16.5± 3.4 in October due to 85 good days and minimum value is 7.4± 2.5 in July due to zero good day. Visibility varies large in July due to 34% coefficient of variance and less in November due to 16% coefficient of variance. Figure 6(a) shows seasonal variation of clearness index (K_T).The Maximum value of K_T is 0.46± 0.09 in pre monsoon (March, April, May) having 170 clear days and minimum value is 0.36± 0.09 in monsoon (June, July, August and September) having 19 clear days. K_T varies large in monsoon due to 25% coefficient of variance and less in post monsoon due to 14% coefficient of variance. Figure 6(b) shows seasonal variation of (L_T). The maximum value of L_T is 2.7± 1.0 in monsoon and minimum value is 1.9± 0.6 in post monsoon (October, November). L_T varies large in winter due to 39% coefficient of variance and less in post monsoon due to 30% coefficient of variance. Figure 6(c) shows seasonal variation of visibility.The maximum value of visibility is 15.2± 2.9 in post monsoon having 135 good days and minimum value is 8.9± 2.4 in winter(December, January, February) having 5 good days. Visibility varies large in monsoon due to 27% coefficient of variance and less in post monsoon due to 19% coefficient of variance. Daily mean of clearness index, Linke turbidity and visibility are fitted in Fourier series equation (8) as shown in figure 7. In figure 7(a), offset for clearness index is 0.55 and amplitude of seasonal component is 0.06. In figure 7(b), offset of Linke turbidity is found 2.5 and amplitude of seasonal component is found 0.2.In figure 7(c), offset of visibility is found 10.4 km and amplitude of seasonal component is found 2.2 km. The annual Linke turbidity is 3.3 to 7.7 in Wuhan(30^{o}32'N, 114^{o}21'E and 30 m a. s. l.), China from 2010 to 2011 [19]. Linke turbidity for four cities of India are found 7.5 for Kolkata (26.93^o N, 88.45^o E,431 m a. s. l.), 4.6 for Poona (18.53^o N, 73.85^o E,559 m a. s. l.), 6.4 for Jaipur (26.93^o N, 88.45^o E, 431 m a. s. l.) and 6.8 for New Delhi (22.65^o N, 88.45^o E, 216 m a. s. l.) on eight years(1993 to 2000)study [20]. The average value of Linke turbidity factor and visibility are found 1.97±

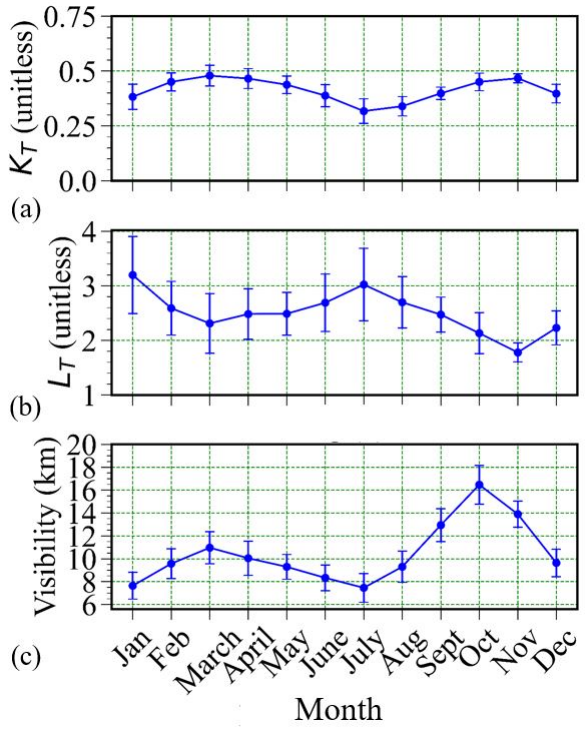

FIGURE 5. Monthly variation of (a) clearness index, (b) Linke turbidity, and (c) visibility.

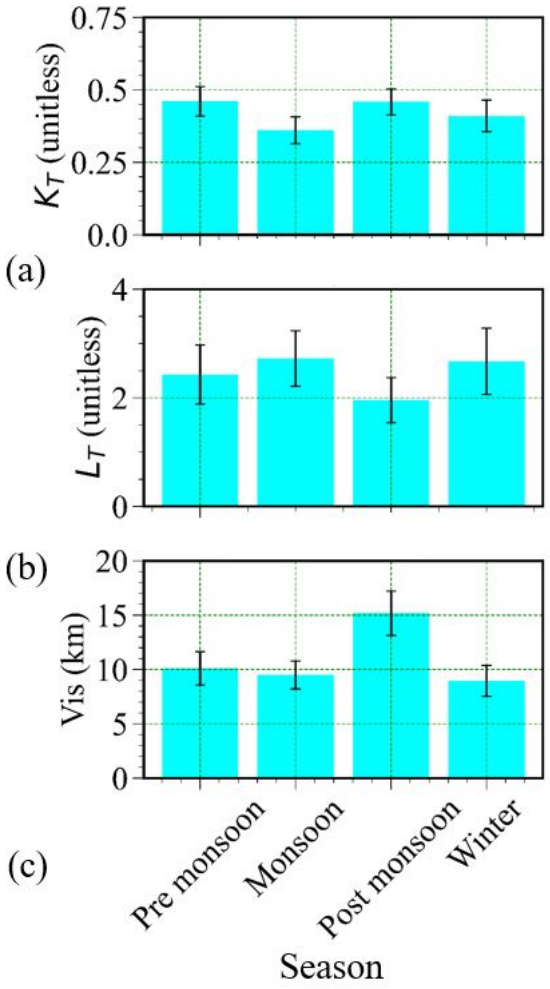

FIGURE 6. Seasonal variation of (a) clearness index, (b) Linke turbidity, and (c) visibility.

0.47 and 28.09 $\pm$ 21.08 km on Jumla (29.28^o N, 82.16^o E and 2300 m a. s. l.) for 2012 [21]. The annual average of visibility is found 18.48 $\pm$ 1.093 km over Jomsom (28.47^{o}N, 83.83^{o}E and 2,700 m a. s. l.) for 2012 [22].The Linke turbidity and visibility were found 5.70 $\pm$ 2.46 and 2.98 $\pm$ 2.13 km over Bode, Bhaktapur (27.68^o N, 85.39^o E, 1297 m a. s. l.) for 2013 [23]. All the above results support to verify our results of Linke turbidity which is closer to the Asian cities. Finally, it is concluded that the level of pollution of Deukhuri valley can be mitigate by using clean energy resources as well as proper management in transportation system and establishment of clean energy based industries as well.

CONCLUSIONS

In 4 year of study period (2015, 2016, 2017, 2018) on Deukhuri Valley of Dang, annual mean for Clearness index (K_T), Linke turbidity index (L_T) and Visibility are observed 0.55 $\pm$ 0.12, 2.5 $\pm$ 1.1 and 10.4 $\pm$ 3.8 km respectively. Number of cloudy days (K_T < 0.34) and number of clear days (K_T > 0.65) are found 106 and 375 respectively. Number of bad days (visibility < 5 km) and number of good days (visibility > 15 km) are found 94 and 188 respectively. About 55 percent of total solar energy incidents on Deukhuri Valley. However Deukhuri valley is favorable to harvest the solar energy and solar related technology can be promoted to substitute the conventional energy like other mega cities in the world.

ACKNOWLEDGMENT

The authors would like to convey our gratitude to faculty of CDP, Patan Multiple Campus, IoST for this opportunity as well as NASA for the data. We sincerely appreciate NAST for the PhD fellowship. We also like to acknowledge Nepal Physical Society (NPS) and Association of Nepali Physicists in America (ANPA) for educational workshop of Python.

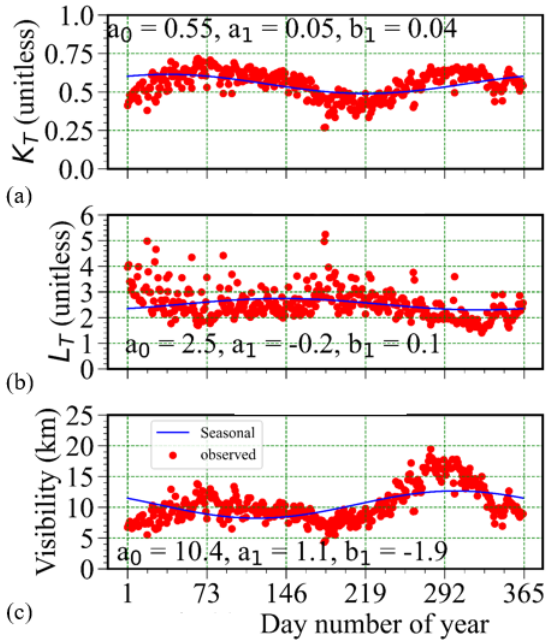

FIGURE 7. Fourier series of (a) clearness index, (b) Linke turbidity and (c) visibility.

EDITORS' NOTE

This manuscript was submitted to the Association of Nepali Physicists in America (ANPA) Conference 2022 for publication in the special issue of Journal of Nepal Physical Society.

REFERENCES

1. I. Purohit and P. Purohit, "Inter-comparability of solar radiation databases in indian context," Renewable and Sustainable Energy Reviews **50**, 735–747 (2015).
2. M. Zhang, B. Wang, D. L. Liu, J. Liu, H. Zhang, P. Feng, D. Kong, J. Cleverly, X. Yang, and Q. Yu, "Incorporating dynamic factors for improving a gis-based solar radiation model," Transactions in GIS **24**, 423–441 (2020).
3. M. R. K. Majupuria T C, *Nepal nature's paradise: insight into diverse facets of topography, flora and ecology* (M Devi,Gwalior,India, 1999).
4. A. Brew-Hammond, "Terminal evaluation of unep gef project solar and wind energy resource assessment—swera," United Nations Environment Programme: Nairobi, Kenya (2011).
5. MoF, *Economic Survey 2018/019* (Ministry of Finance, Government of Nepal, 2018).
6. P. G. Kosmopoulos, S. Kazadzis, H. El-Askary, M. Taylor, A. Gkikas, E. Proestakis, C. Kontoes, and M. M. El-Khayat, "Earth-observation-based estimation and forecasting of particulate matter impact on solar energy in egypt," Remote Sensing **10**, 1870 (2018).
7. C. Gueymard *et al.*, *SMARTS2: a simple model of the atmospheric radiative transfer of sunshine: algorithms and performance assessment*, Vol. 1 (Florida Solar Energy Center Cocoa, FL, 1995).
8. Y. A. Eltbaakh, M. H. Ruslan, M. Alghoul, M. Y. Othman, and K. Sopian, "Issues concerning atmospheric turbidity indices," Renewable and Sustainable Energy Reviews **16**, 6285–6294 (2012).
9. M. Iqbal, *An introduction to solar radiation* (New York: Academic Press, 1983).
10. G. Lothian, "Beer's law and its use in analysis. a review," Analyst **88**, 678–685 (1963).
11. R. H. Inman, J. G. Edson, and C. F. Coimbra, "Impact of local broadband turbidity estimation on forecasting of clear sky direct normal irradiance," Solar Energy **117**, 125–138 (2015).
12. E. Eftimie, "Linke turbidity factor for brasov urban area," Bulletin of the Transilvania University of Brasov. Engineering Sciences. Series I **2**, 61 (2009).
13. H. Horvath, "On the applicability of the koschmieder visibility formula," Atmospheric Environment **5**, 177–184 (1971).
14. L. Chen, B. Yu, Z. Chen, B. Li, and J. Wu, "Investigating the temporal and spatial variability of total ozone column in the yangtze river delta using satellite data: 1978–2013," Remote Sensing **6**, 12527–12543 (2014).
15. L. J. S. Murray R. Spiegel, *Schaum's Outline of Theory and Problems of Statistics (Schaum's Outline Series)* (McGraw-Hill, 1998).
16. CBS, *National Population and Housing Census 2011* (Central Bureau of Statistics, National Planning Commission Secretariat,Government of Nepal, 2011).
17. A. Kudish, D. Wolf, and Y. Machlav, "Solar radiation data for beer sheva, israel," Solar Energy **30**, 33–37 (1983).
18. Y. Hu, L. Yao, Z. Cheng, and Y. Wang, "Long-term atmospheric visibility trends in megacities of china, india and the united states," Environmental research **159**, 466–473 (2017).
19. L. Wang, Y. Chen, Y. Niu, G. A. Salazar, and W. Gong, "Analysis of atmospheric turbidity in clear skies at wuhan, central china," Journal of Earth Science **28**, 729–738 (2017).
20. L. Narain and S. Garg, "Estimation of linke turbidity factors for different regions of india," International Journal of Environment and Waste Management **12**, 52–64 (2013).
21. P. M. Shrestha, I. B. Karki, N. P. Chapagain, and K. N. Poudyal, "Study of linke turbidity factor on solar radiation over jumla," Molung Educational Frontier **9**, 141–149 (2019).
22. P. M. Shrestha, U. Joshi, N. P. Chapagain, I. B. Karki, and K. N. Poudyal, "Study of variation of aerosols on high mountain, jomsom," Molung Educational Frontier **10**, 147–155 (2020).
23. P. Shrestha, N. Chapagain, I. Karki, and K. Poudyal, "Study of linke turbidity factor over bode, bhaktapur," Journal of Nepal Physical Society **6**, 66–73 (2020).